ARI The Bulletin of the Istanbul Technical University VOLUME 54, NUMBER 1
Communicated by Derin Orhon

Flow around Partly Buried Tandem Cylinders in Steady Current

Figen Hatipoğlu and İlhan Avcı
Department of Civil Engineering, Istanbul Technical University, 34469 Maslak, Istanbul, Turkey
(Received 19 November 2003)

This study concerns the flow around a pair of surface-mounted circular cylinders arranged in a tandem configuration. The study comprises (i) flow visualization experiments and (ii) numerical simulations performed by using a CFD model. The influence of the burial ratio, G/D, on flow interference between cylinders is investigated and the lengths of the separation zones are determined for the Reynolds number range varying from 1.3 x $10^4$to 2.6 x 10^4 . Qualitative and quantitative comparsions with experimental results obtained by using the digital image processing technique are made to evaluate the ability of simulation. Results are also compared with the previous studies performed for a single cylinder at corresponding Reynolds numbers. Evidently, the length of the downstream separation zone is influenced by changing burial depth and presence of the upstream cylinder.

Keywords: CFD, circular cylinders, flow visualization, separation zone, tandem configuration.

1. Introduction

Because of being used in many engineering applications such as transmission lines, offshore structures, heat exchangers, circular cylinders have been the subject of research for many years. Regarding the single cylinder, studies were mostly performed about the turbulent flow around the free cylinder and the effects of the wall proximity. See, among others, Achenbach [1], Bearman and Zdravkovich [2], Grass *et al.* [3].

In contrast to single cylinder, there is comparatively few information about flow past multiple cylinders. Early work done by Hori [4] provided an extensive evaluation of flow around parallel circular cylinders. He reported that mutual interference of the two cylinders was stronger in tandem configuration than in the staggered one. The results of a number of investigations were reviewed by Zdravkovich [5, 6] and possible flow regimes for various arrangements of circular cylinders in cross-flow, including the tandem arrangement were classified depending on the longitudinal spacings and Reynolds numbers. Igarashi [7, 8] confirmed these flow regimes for tandem configuration by measuring pressure distrubutions and carrying out flow visualization experiments. Bearman and Wodcock [9], Arie *et al.* [10], Willamson [11] and Sumner *et al.* [12] investigated the effect of interference with multiple cylinders in different configurations by measuring pressure distrubutions and presented in some details.

The development of computational techniques in the past decade has allowed researchers to use computational fluid dynamics, CFD, for application to fluid flow problems. Despite this progress, relatively few investigations have numerically examined on the flow around multiple circular cylinders. Ng and Ko [13] employed discrete vortex method to study the flow around tandem cylinders. Mittal *et al.* [14] investigated the change in the drag coefficient for a pair of cylinders in tandem configuration by using a Petrov-Galerkin velocity-pressure finite element method. Most of these studies have been mainly concerned with the cross-flow around free cylinders and they are mostly restricted by the global features of the flow field such as pressure distribution or forces. According to the author's knowledge no study is yet available which investigates the flow around surface-mounted, partly burried circular cylinders for various burial depth.

Based on the above overview, a study in connection with the application of FLUENT CFD package to the problem of flow around partly burried circular cylinders arranged in tandem configuration is carried out. The accuracy of the CFD scheme is assessed with the aid of values obtained from the flow visualization experiments by using the digital image processing technique. The aims of this study are (i) to describe an application of a CFD model for flow around partly buried cylinders, (ii) to compare CFD output with experimental data derived for the same configuration and flow conditions, and (iii) use these results to discuss the flow interference between the cylin-

ders depending on the burial ratio. Since two cylinders arranged in a tandem configuration are known to behave in a similar way to a single body at small distance ratios, (x/D<1.2-1.8), [5] in order to compare the results with those of single cylinder, the center to center distance ratio has been adopted as x/D=2 for each burial depth in the present study.

2. Numerical Simulation

The governing Reynolds-averaged Navier-Stokes equations for two-dimensional steady state flow for incompressible fluid can be written as:

$$\frac{\partial}{\partial x_i}(u_i) = 0 \tag{1}$$

$$\begin{aligned}\frac{\partial}{\partial x_i}(u_i u_j) &= \frac{\mu}{\rho}\frac{\partial}{\partial x_j}\left(\frac{\partial u_i}{\partial x_j}+\frac{\partial u_j}{\partial x_i}\right) \\ &+ F_i - \frac{1}{\rho}\frac{\partial_p}{\partial x_i} + \frac{\partial}{\partial x_j}\left(-\overline{u_i' u_j'}\right)\end{aligned} \tag{2}$$

where u_i is the velocity in the x_i direction, p is the pressure, μ and ρ are the dynamic viscosity and specific mass of water, F_i represents external forces and the final term represents the Reynolds stresses in Eq. 2.

The description of the Reynolds stresses is one of the main problems in the solution of the Reynolds-averaged Navier-Stokes equations. Several turbulence models for the closure of the problem have been developed recently [15]. In this study, the renormalised group (RNG) k-ε turbulence model has been employed in order to describe Reynolds stresses. The addition of the rate of the strain term in RNG dissipation rate equation allows the RNG model to provide improved predictions in fluid flows involving a large degree of rate strain and boundary curvature [16, 17].

At solid walls, the standart wall-function approach with no slip, impermeable boundary conditions have been employed. The velocity values and turbulence quantities have been prescribed at inlet boundaries using the data measured in the experimental model. Free stream turbulence intensity value has been set as % 5 and the length scale has been specified as %4. For the treatment of water surface, upper boundary has been regarded as a symmetrical boundary. The inlet and outlet lengths have been choosen 5D and 20D respectively to ensure that the fully developed flow

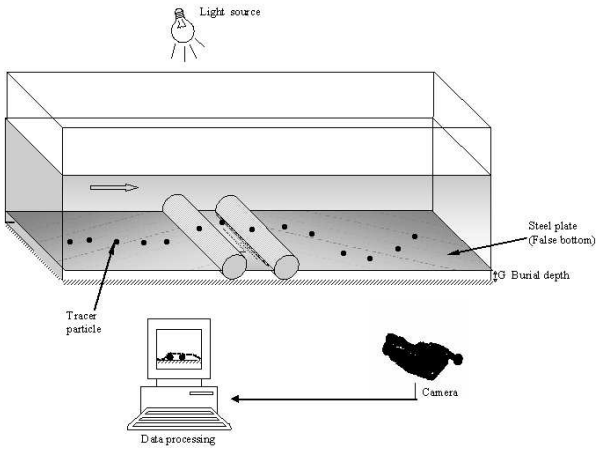

Figure 1. Test setup

was established at the beginning of the cylinder system.

PreBFC V4 structured grid code has been employed to design the mesh. In order to eliminate the effect of the mesh quality, initial tests had been carried out for 500 x 50, 750 x100, 1000x100, 1250 x 200. The numerically predicted streamwise velocities for the two grid sizes of 1000 x100 and 1250 x 200 at the mean depth have differed by %3 and considering the limitation imposed by the available computer capacity, the 1000 x 100 grid was adopted for all calculations.

The commercial CFD software FLUENT 4.5 based on the finite volume technique is employed for the numerical solution of the problem described above. Having set-up the grid and the boundary conditions, then the governing equations have been converted into finite difference equations via integration over control volumes. The Power Law Scheme has been used to discretize the convective terms in space. The discrete equations have been solved under the imposed boundary conditions with an iterative procedure that implements the Line Gauss-Seidel method and the SIMPLE algorithm. A detailed discretization and numerical procedure can be found in the Fluent Manual [18].

3. Experimental Setup and Procedure

The system shown in Fig. 1 consists of a flume, CCD camera (Sony Video Camera Recorder 8 -

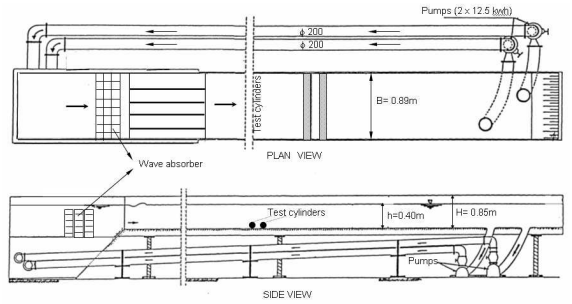

Figure 2. Test flume

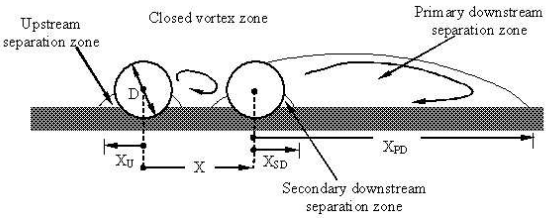

Figure 3. Sketch of flow pattern

F380E), and a PC equipped with a miroVIDEO DC 30 capture card. The recirculating water flume had a working section with a cross sectional area of 0.85 x 0.89 m and a length of 26 m with a smooth bottom (Fig. 2). The test cylinders were fixed and spanned on the base of the flume. The uniform surface roughness of the cylinders (k) was 0.5 mm. The steel plates were used to investigate the effect of different burial ratios (G/D) in the flume. Velocity measurements were carried out by Nixon Instrumentation Stream Flow Velocity Meter, Type 400, Model 403 propeller. The mean velocity of the flow was fixed at U_c=23 cm/s in all experiments. The diameters of the test cylinders and the blokage ratio were 8.9 cm and 10 %, respectively.

A particle of polystyrene with the diameter of 0.4 cm and specific mass of 1.04 g/cm^3 was used as a tracer to visualize the flow pattern. To prevent the interference between the tube and the flow pattern, the particle was released from the tube placed far enough from the upstream cylinder. The movement of the particle was recorded directly to the computer (capturing) with the

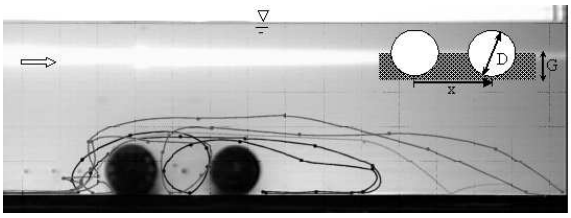

Figure 4. Separation zones for surface mounted tandem clinders,G/D =0, x/D=2

frame rate of 20 frames per second. This treatment was repeated 30-40 times for each burial depth considered. Capturing was performed using Adobe Premiere software package. The capture file was saved as an avi format and played back for analysis. Although there were thirty series in each test condition, seven of the characteristic ones were processed to determine the trajectories of the tracer particle and the lengths of the separation zones.

The experiments cover the determination of the lengths of the separation zones in the cases of wall mounted and partly buried cylinders for steady current. Flow area around the cylinders change with the Reynolds number which was defined as follows:

$$Re = \frac{U_c(D-G)}{\nu} \tag{3}$$

where D, G, ν and U_c are diameter of the cylinders, burial depth of the cylinders, kinematic viscosity of fluid and mean velocity at top level of the cylinders respectively.

4. Results and Comparison with Predictions from Numerical Model

The results of the simulation are consistent with the flow structures observed in the experiments. As mentioned before the presence of the cylinder system, approaching flow is divided into upward and downward flows. The downward flow forms an eddy on the front face of the upstream cylinder while the upward flow is separated from the upstream cylinder. Separated flow goes onto the downstream cylinder with an unstable reattachment and forms the largest separation zone behind the downstream cylinder (Fig. 3). The seperation zone in front of the upstream cylinder is small and reduce in size with increasing burial

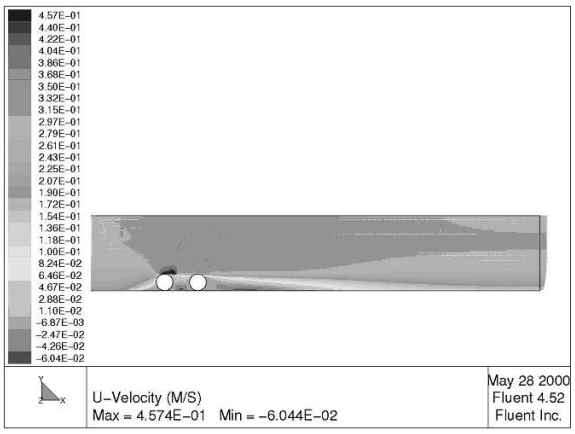

Figure 5. Simulated separation zones for G/D=0, x/D=2

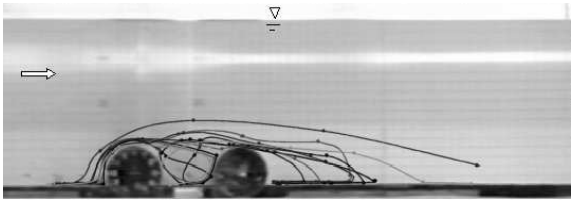

Figure 6. Separation zones for G/D=0.20 and x/D=2

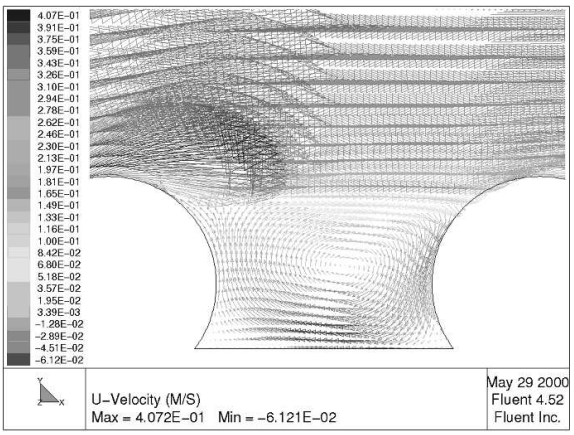

Figure 7. Closed vortex zone for tandem cylinders in case of G/D=0.20, x/D=2

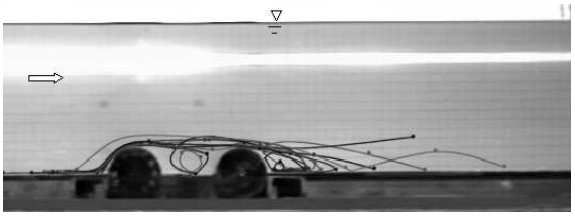

Figure 8. Separation zones for semi buried tandem cylinders, G/D=0.50, x/D=2

ratio. A closed vortex zone between the cylinders and small bubles in the upstream and the downstream sides of the contact points of the cylinders are observed.

Fig. 4 represents the experimental result obtained by using image processing technique for surface mounted case. The lengths of the upstream and downstream separation zones are measured as 1.1 D and 4.4 D. Fig. 5 shows the predicted streamwise velocity pattern for the same case. It can be seen that the presence of the cylinders generate significant local high velocities. These velocities generated above the cylinders represent the form drag effect which is introduced by the cylinders causing fluid acceleration and deceleration. From the velocity pattern, the locations where the separated flow reattaches to the wall can be easily identified. The lengths of the primary separation zones are predicted as 1.3D and 6.5D for the upstream and downstream regions respectively. Comparable results have been reported for the surface mounted single cylinder by several authors. The lengths of the separation regions have been predicted in range between 0.77D [19] and 0.98D [20] for the upstream and 7.8D [19] 9D [20] for the downstream respectively.

The lengths of the separation zones, for the case of G/D=0.20, are found as 0.7D for upstream and 3.5D for downstream by experiment (Fig. 6) and 0.9D for upstream and 4.3D for downstream by simulation (Fig. 7). These values has been predicted as 0.9D and 6.7D those for single cylinder case [21].

In the semi buried case (G/D=0.50) the length of the downstream separation zone has established as 2.2D by experiment (Fig. 8) and 1.8D

Table 1
Experimental and Numerical Results

	$\frac{X}{D}$	$\frac{G}{D}$	$Re = \frac{U_c(D-G)}{\nu}$	The length of the upstream separation zone (X_U)	The length of the primary downstream separation zone (X_{PD})	The length of the secondary downstream separation zone (X_{SD})
Experimental	2	0	26700	$1.1D$	$4.4D$	–
results	2	0.20	21360	$0.70D$	$3.5D$	–
	2	0.50	13350	–	$2.2D$	–
Numerical	2	0	26700	$1.3D$	$6.5D$	$0.8D$
results	2	0.20	21360	$0.90D$	$4.3D$	$0.6D$
	2	0.50	13350	–	$1.8D$	–

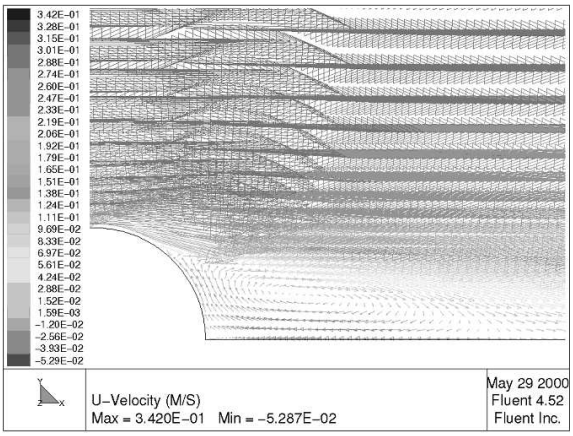

Figure 9. Simulated primary downstream separation zone for G/D=0.50, x/D=2

by simulation (Fig. 9). The corresponding value for upstream could not be defined since it was too small. For single cylinder case this value predicted as 2.1D [21]. Although present study is mainly focused on the primary separation zones, the lengths of the secondary downstream separation zones are also predicted and presented all together with the other results in Table 1.

5. Conclusion

The effects of the different burial ratios, G/D, on flow interference between circular cylinders arranged in tandem configuration was investigated by CFD simulation. Outputs from the simulation were compared with the experimental results obtained by using digital image processing technique.

It was found that the lengths of the separations zones decreased with the increasing burial ratios. By comparing present results with the reported results obtained for the single cylinder case, it can be concluded that the perturbation introduced by the upstream cylinder significantly reduces the lengths of the downstream separation zones.

The results of the simulation are consistent with the flow structures observed in the experiments. However the lengths of the separation zones were overpredicted by about in the range 20-30% depending on the burial ratio. The largest discrepancy was found for the surface mounted case. This overprediction may be attributed to usage of structured mesh which can lead to reduction of the mesh flexibility and the adaptation capability in the zones with high skewness.

The results have implications both for providing data for future correlations and contributing to understanding of the gross flow behaviour around surface mounted and partly buried circular cylinders arranged in tandem configuration.

6. Acknowledgements

The authors would like to thank to the Scientific and Technical Research Council of Turkey (TUBITAK) and Istanbul Technical University Research Fund for their financial support.

References

[1] E. Achenbach, J. Fluid Mech **34**, 625 (1968).
[2] P.W. Bearman and M.M. Zdravkovich, J. Fluid Mech. **189**, 33 (1978).
[3] A.J. Grass, P.W.J. Raven, R.J. Stuart, and J.A. Bray, J. Energy Resources Tech. **106**, 70 (1984).
[4] E. Hori, Experiments on flow around a pair

of parallel circular cylinders, Proc. 9th Japan National Congress for Applied Mech., Tokyo (1959).
[5] M.M. Zdravkovich, ASME, Journal of Fluids Engineering **99**, 618 (1977).
[6] M.M. Zdravkovich, Journal of Fluids and Structures **1**, 239 (1987).
[7] T. Igarashi, Bulletin of JSME **24**, 323 (1981).
[8] T. Igarashi, Bulletin of JSME **27**, 2380 (1984).
[9] P.W. Bearman and A.J. Wadcock, J. Fluid Mech. **61**, 499 (1973).
[10] M. Arie, M. Kiya, M. Moriya, and H. Mori, ASME, Journal of Fluids Engineering **105**, 161 (1983).
[11] C.H.K. Willamson, J. Fluid Mech. **159**, 1 (1985).
[12] D. Sumner, S.S.T. Wong, S.J. Price, and M.P.Paidoussis, Journal of Fluids and Structures **13**, 309 (1999).
[13] C.W. Ng and N.W.M. Ko, Journal of Wind Engineering and Industrial Aerodynamics **54/55**, 277 (1995).
[14] S. Mittal, V. Kumar, and A. Raghuvanshi, International Journal for Numerical Methods in Fluids **25**, 1315 (1997).
[15] C.G. Speziale and R.M.C. So, Turbulence modelling and simulation (CRC Press and Springer-Verlag, USA, 1998).
[16] T.B. Gatski, M.Y. Hussaini, and J.L. Lumney, Simulation and Modelling of Turbulent Flows (Oxford University Press, New York, 1986).
[17] S.H. Lam, Physics of Fluids **4**, 1007 (1992).
[18] FLUENT User's Guide, Version 4.3 (Fluent incorporated, Lebanon, NH:Central Resource Park, 03766, 1995).
[19] B. Brors, J. Hydraulic Engineering **125**, 511 (1999).
[20] T. Solberg, Dr.Ing.thesis, University of Trondheim, NTH (1992).
[21] F. Hatipoğlu and I. Avcı, Ocean Engineering **30**, 239 (2003).